Rev. Cubana Fis. **42**, 58 (2025) COMUNICACIONES ORIGINALES

# CORRELATING TEXTURE AND ELECTROMECHANICAL PROPERTIES OF ACTIVATED CARBONS: FIRST STEPS

## CORRELACIONANDO TEXTURA Y PROPIEDADES ELECTROMECÁNICAS DE CARBONES ACTIVADOS: PRIMEROS PASOS

H. Reborido[a†], R. Machado-García[b], D. Cascaret-Carmenaty[b], O. Quesada-González[b], P. Muné[a†]

a) Departamento de Física, Universidad de Oriente, Cuba. mune@uo.edu.cu[†]
b) Departamento de Química, Universidad de Oriente, Cuba
† corresponding author

Recibido 10/11/2024; Aceptado 21/2/2025

Keywords: Porous materials (Materiales porosos); Activated carbons (Carbones activados); Electrical conductivity (Conductividad eléctrica); Mechanical properties (Propiedades mecánicas).

The growing demand for activated carbons has driven the development of inexpensive and easily applicable experimental methods for evaluating their behavior. One promising avenue, for the obtaining of activated carbon, lies in utilizing agro-industrial residues. This approach offers a sustainable path to minimize environmental impact while producing high-value materials from affordable sources [1,2].

This note presents a simple experimental method for determining four electromechanical parameters of powdered activated carbon samples. These parameters are then used to derive a mathematical expression describing the dependence of sample conductivity on applied uniaxial pressure. Furthermore, the note shows evidence of a certain correlation between some of these parameters and the texture of the activated carbon samples.

For electrical characterization of the activated carbon a two-point method was used. A known mass of material was compacted uniaxially (~ 50 mg) under increasing pressures within an insulating matrix using piston and base electrodes. An ohmmeter was used to measure the electrical resistance across the electrodes at 29 °C [3]. This study focuses on the ratio of density to resistivity $\rho_m/\rho$, a parameter that can be determined using the expression:

$$\frac{\rho_m}{\rho} = \frac{m}{R \cdot A^2} \tag{1}$$

Here $m$ represents the mass of the carbonaceous material, $R$ is the electrical resistance and $A$ is the cross-sectional area. This ratio exhibits a linear relationship with uniaxial pressure applied to the carbonaceous powder, particularly in the range of 20-240 MPa. Moreover, this parameter offers the advantage of being independent of uncertainties associated with measuring the distance between contacts.

At this point, the linear relationship between the parameter and uniaxial pressure, focusing on carbonaceous materials derived from various sources is explored. Figure 1 illustrates this linear dependence. Let us see first the obtention of the carbonaceous materials derived from sugar cane bagasse. In this case three samples were prepared. Two were treated with acid and base, respectively, while one remained untreated. Treatments involved a 24-hour impregnation in 0.5 mol/L activating agent solution, followed by washing with distilled water and drying at 105 °C. All samples were then subjected to pyrolysis at 850 °C in an argon flux of 5 mL/min for 30 minutes and cooled down to room temperature in the same argon flux. The resulting material from the pyrolysis was washed in deionized water using ultrasound with a power of 40 W during 5 minutes. Despite these differences in treatment, the parameter consistently displays a linear behavior with applied uniaxial pressure. Similar linear behavior was also observed in carbonaceous materials derived from other agro-industrial residuals, namely coconut shells, peanut hulls, and rice husks (see Figure 1). These materials were first transformed into black carbon through pyrolysis at 600 °C in a nitrogen flux of 80 mL/min. Subsequently, all carbons were physically activated using steam at 850 °C for 30 minutes. As last step, the resulting material was cooled down until ambient in the same nitrogen flux. The studied powders had similar particle size; it was less than 63 in all samples. Linear least-squares fitting of the experimental data yielded high correlation coefficients ($r^2 > 0.99$), confirming a strong linear relationship in all cases. Uncertainties in the intercept and slope were below 4 %.

On the other hand, the effective-medium approximation (EMA) provides a framework for understanding the effective conductivity $\sigma_e$, of porous materials, such as those studied here. Equation (2) describes the effective conductivity of the porous material, where represents the conductivity of the carbonaceous matrix and $c$ is the pores concentration [4]:

$$\sigma_e = \sigma_B\left(1 - \frac{3}{2}c\right) \tag{2}$$

Here $c < 3/2$ , indicating that the percolation threshold has been exceeded.

The sample volume exhibits an exponential dependence on the uniaxial pressure, as described by (3):

$$V = A_1 e^{-\beta_1 P} \tag{3}$$

where $P$ represents the uniaxial pressure, $A_1$ is the volume at zero pressure and $\beta_1$ is the compressibility coefficient [5].

Experimental data presented in Figure 1 can be described by the following expression:

$$\frac{\rho_m}{\rho}(P) = A_2 + \beta_2 P \tag{4}$$

Combining (3) and (4) allows us to express the sample electrical conductivity as a function of pressure, as shown in equation (5):

$$\sigma_e = \frac{1}{m}\left(A_2 + \beta_2 P\right) A_1 e^{-\beta_1 P} \tag{5}$$

This relationship suggests that uniaxial pressure has two opposing effects on the electrical conductivity of the sample. At lower pressures, the electrical conductivity increases with pressure due to improved contact between the grains. Higher pressures, however, lead to grain fracture and consequently a decrease in conductivity.

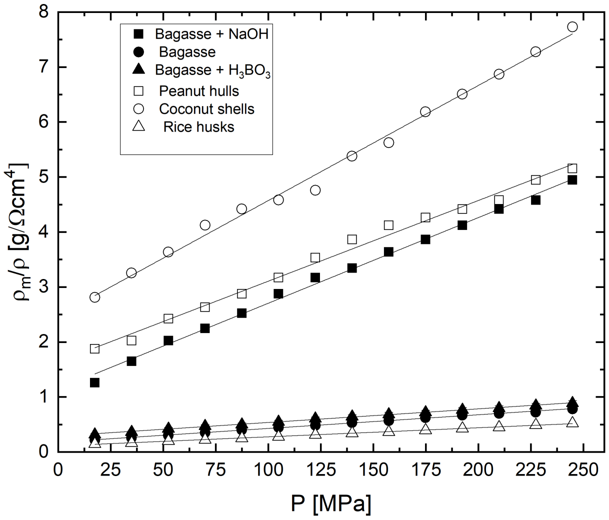

Figure 1. $\frac{\rho_m}{\rho}(P)$ dependence of different carbonaceous materials derived from sugar cane bagasse and others agro-industrial residuals. The continue lines represent the linear fittings of the experimental data obtained by least squares method.

Figure 2 presents both experimental data and theoretical calculations, using (5), for the dependence of effective conductivity on uniaxial pressure. The inset illustrates the procedure for determining $\beta_1$ and $A_1$ starting from the linear behavior of $\ln(V)$ as a function of uniaxial pressure. Also, this figure shows increasing uncertainty with pressure in the experimental data for coconut shell and peanut hull samples. A few data points (two or three per sample) deviate significantly from (5), even accounting for experimental uncertainty. This deviation is likely due to the empirical nature of (5) and uncertainties in parameters $A_1$, $\beta_1$, $A_2$, and $\beta_2$ (below 1 % and 5 %, respectively, for $A_1$ and $\beta_1$). The equation (5) also predicts a maximum of $\sigma_e(P)$ at $P_{max} = \frac{1}{\beta_1} - \frac{A_2}{\beta_2}$, which can be observed, for the sample derived from peanut hulls, into the pressure range of the measure.

Equation (6) enables the determination of the electrical conductivity of the carbonaceous material, $\sigma_B$, independent of pore effects. This aspect is crucial for evaluating the suitability of activated carbons for electrical applications:

$$\sigma_e\left(P \to 0\right) = \frac{A_1 A_2}{m} = \sigma_B\left(1 - \frac{3}{2}\frac{V_p}{A_1}\right) \tag{6}$$

Here $V_p$ represents the pore volume linked to meso and macropores.

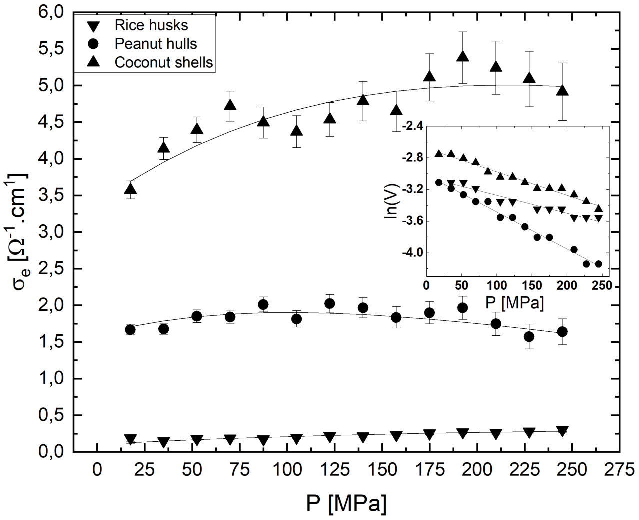

Figure 2. Effective conductivity as a function of the uniaxial pressure for carbonaceous materials obtained from the biomass described in the legend. The solid lines represent the conductivity values calculated using equation (5). The inset depicts the linear relationship between natural logarithm of volume and pressure, which confirms Equation (3).The error bars represent the experimental uncertainties.

Due to the small size of micropores, they are considered as part of the carbonaceous matrix. The pore volume, $V_p^*$, is usually determined by means of adsorption and desorption of nitrogen ($N_2$) by the carbonaceous material and it is given in cm$^3$/g. However, in (6), $V_p = mV_p^*$, where $m = 50$ mg . In addition, the mathematical expression $P \to 0$ refers the limit of low pressures, where the linear and exponential dependencies on $P$ are satisfied.

Table I provides an example of applying (6) to samples with effective electrical conductivity as a function of uniaxial pressure, as depicted in Figure 2. The results indicate that the sample derived from coconut shells exhibits the highest value of $\sigma_B$, followed by the sample derived from peanut hulls. The sample obtained from rice husks demonstrates the least desirable behavior due to its lowest value of $\sigma_B$. This observation aligns with the presence of a significant percentage of $SiO_2$ in the carbonaceous materials obtained from rice husks [2]. Also, it is easy of verifying for all samples $\frac{V_p}{A_1} < 0.16$ that satisfies the condition predicted by EMA.

Table 1. $V_p$, $A_1$, $A_2$, and $\sigma_B$ of the samples presented in Figure 2.

| Biomass | $V_p$ [cm$^3$] | $A_1$ [cm$^3$] | $A_2 \left[\frac{g}{\Omega\,\mathrm{cm}^4}\right]$ | $\sigma_e \left[\frac{1}{\Omega\,\mathrm{cm}}\right]$ |
|---|---|---|---|---|
| Coconut shells | 0.0104 | 0.068 | 2.48 | 4.39 |
| Peanut hulls | 0.0056 | 0.049 | 1.64 | 1.93 |
| Rice husks | 0.0035 | 0.048 | 0.110 | 0.12 |

In summary, this study has successfully derived an expression for the dependence of effective conductivity, $\sigma_e$, on uniaxial pressure, $P$, leveraging the linear relationship between the product of density and conductivity, $\rho_m\sigma_e$, and pressure, alongside the established relationship between sample volume and applied uniaxial pressure. The four parameters in (5) provide a unique ”fingerprint”for characterizing the electro-mechanical properties of activated carbons. This finding suggests that the methodology employed in this study holds promise for evaluating the textural properties of activated carbons, serving as a valuable preliminary assessment tool. A series of ongoing research projects aim to further explore this approach, potentially leading to a more comprehensive understanding of the relationship between texture and electro-mechanical behavior in activated carbons.

## REFERENCES

[1] Z. Heidarinejad, M. Hadi Dehghani, M. Heidari, I. A. Mika Sillanpää, *Environ. Chem. Lett.*, **18**, 393 (2020).

[2] R. G. Machado-García, “Synthesis of composites based on activated carbon and $TiO_2$ doped with Co and Fe from residues for the photocatalytic degradation of Cibacron yellow F-4G dye”, PhD. Thesis, Universidad de Oriente (2022).

[3] V. N. Rubchevskiy, S. A. Ovchinnikova, Yu. A. Chernyshov, I. V. Zolotarev, Yu. A. Yatsenko, E. I. Toryanik, A. V. Gryzlov, and S. S. Kubrak, *Coke Chem.*, **57**, 381 (2014).

[4] D. Stroud, *Phys. Rev. B*, **12**, 8 (1975).

[5] N. Warren, *J. Geophys. Res.*, **78**, 352 (1973).

---